Pedosphere **36**(2): 511–526, 2026
doi: 10.1016/j.pedsph.2025.01.003
ISSN 1002-0160/CN 32-1315/P
© 2026 Soil Science Society of China
Published by Elsevier B.V. and Science Press

PEDOSPHERE

www.elsevier.com/locate/pedosphere

Unearthing potential of aluminum-modified biochar for saline-alkali soil rejuvenation and microbial diversity enhancement

Saba BABAR[1], Amanullah BALOCH[2], Muhammad QASIM[1], Jiyuan WANG[1], Xiangling WANG[1], Rashid IQBAL[3,4], Ali M. ABD-ELKADER[1], Khurram SHEHZAD[5], Xiaoyang XIA[1] and Cuncang JIANG[1,*]

[1]*Microelement Research Center, College of Resources and Environment, Huazhong Agricultural University, Wuhan 430070 (China)*
[2]*National Key Laboratory of Crop Genetic Improvement and College of Plant Science and Technology, Huazhong Agricultural University, Wuhan 430070 (China)*
[3]*Department of Agronomy, Faculty of Agriculture and Environment, The Islamia University of Bahawalpur, Bahawalpur 63100 (Pakistan)*
[4]*Department of Life Sciences, Western Caspian University, Baku AZ1001 (Azerbaijan)*
[5]*Hubei Key Laboratory of Soil Environment and Pollution Remediation, College of Resources and Environment, Huazhong Agricultural University, Wuhan 430070 (China)*

(Received September 20, 2024; revised November 9, 2024; accepted January 2, 2025)

ABSTRACT

Saline-alkali soils pose a serious challenge to the agricultural production system. Although ordinary biochar application has been found to be beneficial in mitigating salt stress, its effectiveness could be further enhanced through some modifications. In this study, a soil column leaching experiment was conducted to evaluate the potential roles of original rice straw biochar (OB) and aluminum-modified rice straw biochar (AB) in the reclamation of a saline-alkali soil. Five treatments were designed: treatments amended with 1% and 3% (weight:weight) OB and AB (1% OB, 3% OB, 1% AB, and 3% AB, respectively) and without biochar (control, CK), and each treatment was repeated four times under a completely randomized design. The results reflected that the 3% AB treatment was more effective than other treatments in reducing soil pH, electrical conductivity, sodium adsorption ratio, and exchangeable sodium ions (by 7.8%, 27.4%, 36.8%, and 30.2%, respectively, relative to CK). It was mainly due to the maximum replacement of sodium ions with aluminum ions on soil exchange sites. Additionally, irrigation practices further accelerated the salt removal from the soil column *via* leaching. With a reduction in salt content, soil β-1,4-glucosidase and β-cellobiohydrolase activities became enhanced, particularly in the 3% AB treatment. Notably, biochar application also altered soil microbial community composition. The relative abundance of salt-tolerant bacteria, such as Proteobacteria and Actinobacteriota, was greatly improved in the 3% AB-amended soil, thereby benefiting soil health. In conclusion, this study proves the multiple enhanced impacts of AB on overall soil properties and also provides new insight into the utilization of natural resources with slight modification for reclaiming saline-alkali soils.

Key Words: enzyme activity, microbial community, reclamation, salinization, salt leaching, salt stress

Citation: Babar S, Baloch A, Qasim M, Wang J Y, Wang X L, Iqbal R, Abd-Elkader A M, Shehzad K, Xia X Y, Jiang C C. 2026. Unearthing potential of aluminum-modified biochar for saline-alkali soil rejuvenation and microbial diversity enhancement. *Pedosphere*. **36**(2): 511–526.

INTRODUCTION

Soil salinization is a major agricultural constraint that converts agronomically useful areas into nonproductive land, affecting 1%–2% of agricultural land area annually (Sahab *et al*., 2021). This problem is more prevalent in arid and semi-arid regions with low average annual precipitation (Navarro-Torre *et al*., 2023). More than 30% of the world's salinized area is located in China, out of which one-third is in Xinjiang (Liang *et al*., 2021). High concentrations of soluble salts, particularly sodium ions (Na^+) in the saline-alkali soil, negatively affect soil physicochemical properties by degrading soil structure and lowering soil organic matter (SOM) and nutrient contents (Saifullah *et al*., 2018; Tian *et al*., 2023). All these changes, in turn, severely affect crop growth and cause an annual worldwide economic loss of about 27.2 billion dollars in agricultural production (Elmeknassi *et al*., 2024). In addition, soil salinity also induces a detrimental impact on soil biological properties by decreasing the diversity and abundance of microbial community, which plays an important role in nutrient cycling (Haj-Amor *et al*., 2022; Yang *et al*., 2023). It is expected that the global population will increase to 10 billion by 2050, and the current arable land is insufficient to meet the food demand of the increasing population (Zul Azlan *et al*., 2024). Therefore, to cope with this problem, it is necessary to bring the saline-alkaline land under cultivation by adopting control measures that could effectively mitigate the salt stress, improve soil fertility status, and promote sustainable agriculture.

Recently, biochar application has received great attention as an effective strategy to remediate the saline-alkali soil and sustain crop productivity (Sánchez *et al*., 2022; Han *et al*., 2023). Biochar, a carbonaceous material produ-

*Corresponding author. E-mail: jcc2000@mail.hzau.edu.cn.

ced under anaerobic conditions, has a porous structure and large specific area (Lu *et al*., 2023; Wang *et al*., 2025). It contains numerous functional groups such as –COOH, –OH, C=O, phenolic –OH, and –CHO groups, which play an important role in soil nutrient adsorption such as potassium (K^+), ammonium (NH_4^+) and calcium (Ca^{2+}) ions, thus improving soil fertility status (Zhang C *et al*., 2023; Adhikari *et al*., 2024). Biochar addition modifies soil physicochemical properties by regulating soil pH and increasing SOM, cation exchange capacity (CEC), porosity, aggregate stability, and saturated hydraulic conductivity, as well as retaining essential nutrients in the soil (Duan *et al*., 2023; Wang K *et al*., 2024). Biochar amendment is mostly used in acidic soils, where it indicates more pronounced positive effects on soil properties, but its utilization in saline-sodic soils is very limited due to the alkaline nature. Nowadays, modified biochar, such as acidic or cationic modified biochar, is used to increase its efficiency in reclaiming saline-alkali soil by displacing Na^+ from soil exchange sites with divalent cations (He *et al*., 2023; Che *et al*., 2024). Several studies have reported the beneficial effect of acidified/cationic biochar in reclaiming saline-alkali soil (Zhou *et al*., 2021; Singh *et al*., 2023) by increasing soil moisture content, forming soil water-stable macro-aggregates, and facilitating the Na^+ adsorption on biochar surface (Zhou *et al*., 2021; Gao *et al*., 2024). Additionally, modified biochar as a nutrient-enriched carrier and modifier releases more K^+, Ca^{2+}, and magnesium ions (Mg^{2+}), causing the displacement of Na^+ from soil exchange sites into soil solution (Zhao *et al*., 2020; Wang *et al*., 2025).

Furthermore, emerging evidence indicates that modified biochar with metal salts, such as chlorides of Ca, Mg, iron (Fe), *etc*., can induce a shift in pH from high alkalinity to lower acidity (Li C Y *et al*., 2023; Li H *et al*., 2023; Peng C *et al*., 2023; Che *et al*., 2024). This transformation not only enhances soil CEC by displacing Na^+ from soil exchange sites, but also allows the salts to leach out of the soil profile with irrigation practices (Xu *et al*., 2023). Such improvements in soil physicochemical properties with the application of modified biochar produce a well-pronounced positive effect on soil microbial diversity, community composition, and enzyme activities, which play a crucial role in improving soil health and ecosystem functioning (He *et al*., 2023; Bolan *et al*., 2024). In earlier investigations, the application of Ca- and Fe-based modified biochar significantly improved bacterial diversity, bacterial population size, and various enzyme activities that help in nutrient cycling and overall improve soil health (Peng *et al*., 2022; Wang *et al*., 2023). Despite the advancement in this research, a knowledge gap still persists regarding the effects of modified biochar in reclaiming saline-sodic soils.

Aluminum ions (Al^{3+}) have a high charge density and better binding affinity to displace Na^+ from exchange sites and release them into soil solution (Qian and Chen, 2014). Consequently, these Na^+ ions from soil solution are leached out with irrigation water. In addition, Al^{3+} reacts with other soil constituents, such as organic matter and other dissolved ions, and forms inorganic complexes and aluminum (Al) hydroxides, which neutralize soil alkalinity (Aide, 2022). In previous studies, Al-modified biochar (AB) was used for the remediation of arsenic-contaminated acidic soils (He *et al*., 2020) and chromium-containing wastewater (Yang *et al*., 2022). Their effectiveness was mainly attributed to several factors, such as large surface area, additional functional groups, electrostatic attraction, redox potential, and complex formation (Zheng *et al*., 2020). Notably, AB exhibits a strong selective ion-adsorption capacity due to the Al oxide coating, which increases its affinity for Na^+ and can effectively replace Na^+ from exchange sites (Aide, 2022; Li C Y *et al*., 2023). Meanwhile, it releases essential nutrients like Ca^{2+} and Mg^{2+}, which can also contribute to the reclamation of soil alkalinity (Porras *et al*., 2017; Patrick *et al*., 2022). In contrast, ordinary biochar possesses a low selective ion-adsorption capacity and pH buffering capacity due to its reduced surface area, CEC, and alkaline properties (Hameed *et al*., 2024). Interestingly, AB offers a more stable and prolonged beneficial impact on improving soil properties and fostering microbial activity, thereby reducing the ecological disturbance linked to chemical application. Thus, these multiple benefits can make AB an effective amendment for ameliorating saline-alkali soils.

The objectives of this study were to 1) evaluate the potential of AB in reclaiming the saline-sodic soil along with successive irrigation practices, 2) enumerate the alterations in soil chemical properties and enzyme activities, and 3) explore the differences in microbial composition and diversity after salt leaching between the soils amended with AB and original rice straw biochar (OB). We hypothesized that the application of AB and subsequent leaching with irrigation water could accelerate the reclamation process compared to the individual application of OB. Moreover, we hypothesized that AB could modify soil chemical and biological properties, which would be beneficial for soil health and promote sustainable agriculture.

MATERIALS AND METHODS

Biochar preparation and characterization

Biochar used in the current study was produced from pyrolysis of rice straw at 500 °C for 2 h under N_2 atmosphere, which was provided by Hubei Academy of Agricultural Sciences, Wuhan, Hubei Province, China (114°32′ E, 30°48′ N). Before application, the original rice straw biochar (OB) was first air-dried, crushed, and passed through a 0.85-mm sieve. Aluminum-modified biochar (AB) was prepared from OB using the impregnation and calcination

method (Wang *et al*., 2023). The basic properties of OB and AB are shown in Table SI (see Supplementary Material for Table SI). The surface morphology and microscopic attributes of biochar were determined by scanning electron microscopy (SEM). Meanwhile, the elemental contents on the biochar surface, such as C (carbon), O (oxygen), Ca, Mg, K, Na, and Al, were measured by an energy dispersive spectrometer (EDS). Additionally, a Fourier transform infrared (FTIR) spectrometer (Nicolet IS50, Thermo Scientific, USA) was used to identify surface functional groups on biochar. The X-ray diffraction (XRD) patterns of biochar powder were obtained by an X-ray diffractometer (D8 Advanced, Bruker Co., USA) using a CuK_α radiation beam ($\lambda = 0.150$ 45 nm) in a diffraction tube of 40 kV voltage and 40 mA current with a scanning rate of 10° min^{-1} and scanning range of 5°–90°.

Test soil and leaching experiment

The soil used in this study is a saline-alkali soil that was collected from Aral City, Xinjiang, China (81°29′ E, 40°54′ N). The soil was air-dried and sieved through a 2-mm mesh to remove plant residues and pebbles. The basic properties of this soil were determined as follows: pH 9.90, electrical conductivity (EC) 4 958.67 μS cm^{-1}, and SOM 2.98 g kg^{-1}. A leaching experiment was conducted in a greenhouse at Huazhong Agricultural University, Wuhan, Hubei Province, China (114°22′ E, 30°29′ N), to evaluate the effects of biochar and irrigation water on the reclamation of saline-alkali soil. Five treatments were designed: treatments amended with 1% and 3% (weight:weight) OB and AB (1% OB, 3% OB, 1% AB, and 3% AB, respectively) and without biochar (control, CK), and each treatment was repeated four times in a completely randomized design. Plastic containers with a diameter of 8 cm and a length of 20.5 cm were used to conduct the leaching process. The column contained a big hole (2.5 mm in diameter) at the bottom that was covered with a layer of filter paper and 80-mesh nylon. For uniform leaching, a layer of quartz sand was laid up to 2 cm depth on the filter paper. On the top of sand layer, the saline-sodic soil samples (*ca*. 1.5 kg) amended with and without biochar were added, and soil surface was levelled after the addition of each soil sample. Three layers of filter paper were placed on the top of soil sample to avoid soil surface disturbance and splashing during water addition. The container was attached to a glass storage bottle. The soil columns were saturated with distilled water to maintain 60% of water-holding capacity. Then, they were incubated for 15 d at room temperature to facilitate better interaction between soil and biochar. After 15 d, a constant quantity of water was added to the container in the following manner. At a time each day, 50 mL of distilled water was added for 4 consecutive days and then left for 3 d for better percolation through the soil column and effective salt removal. The leachate was collected every week for analysis by replacing the leachate collection container (*i.e*., the glass storage bottle). The same pattern was followed during the whole leaching experiment. Four leachates were collected at different time intervals on days 8, 16, 24, and 32 and then used to determine the pH, EC, and the contents of water-soluble cations such as Na^+, K^+, Ca^{2+}, and Mg^{2+} in the leaching solution. The duration of the whole experiment was about 72 d.

The basic purpose of the experimental leaching model was to simulate field-relevant leaching practices that could be adapted in salt-affected soils of the arid region in Xinjiang, where inadequate rainfall distribution, high evaporation rate, and great fluctuations in temperature inhibit the natural salt leaching (Liang *et al*., 2021; Ding *et al*., 2023). In addition, the amount of water used in this study was based on the typical irrigation practices, which can stimulate a realistic leaching process for saline-alkali soils (Zhang Y *et al*., 2020; Xiao *et al*., 2022). Meanwhile, different time sets of leachate collection allow us to better understand time-dependent interactions between biochar and soil environment, especially in terms of salt removal efficiency (Liu *et al*., 2023; Wang *et al*., 2025). Thus, under controlled conditions, a detailed assessment of salt removal by leaching action reflects how irrigation practices and soil treatments function in real-world scenarios and mitigate soil salinity issues in regions facing a similar environmental challenge.

Soil sample collection and analysis

Before soil sample collection, the soil column was standing for 25 d to reach a constant state. Afterwards, the soils from four replicates of each treatment were homogeneously mixed in a big pot to get a composite sample. The collected soil sample was divided into three parts. One part was kept at −20 °C for the determination of extracellular enzyme activity, while the second part was stored at −80 °C for analyzing soil microbial sequence. Soil physicochemical properties were determined by the methods of Bao (2000). Soil pH was determined by a pH meter (FE20, Mettler Toledo, China) at a soil:water ratio of 1:2.5 (weight/volume), while soil EC was measured at a soil:water ratio of 1:5 (weight/volume) at 25 °C (Chen *et al*., 2021; Wang *et al*., 2025). The SOM content was measured using the potassium dichromate ($K_2Cr_2O_7$) volumetric method. Soil water-soluble and exchangeable Na^+, K^+, Ca^{2+}, and Mg^{2+} were extracted with ultrapure water at a ratio of 1:5 (weight/volume) and 1 mol L^{-1} CH_3COONH_4, respectively, and then determined using a flame photometer (FP6410, Shanghai Jingqi Instrument Co., Ltd., China) and a flame atomic absorption spectrophotometer (204DUO, Agilent, USA), respectively. Soil extracellular enzyme activities were determined following the protocol mentioned by Wang X L *et al*. (2024a).

The sodium adsorption ratio (SAR) was calculated based on the following formula (Qadir *et al*., 2021):

$$\mathrm{SAR} = \mathrm{Na}^{+} / \sqrt{\frac{1}{2}(\mathrm{Ca}^{2+} + \mathrm{Mg}^{2+})} \quad (1)$$

Soil DNA extraction and high-throughput sequencing

Soil DNA was extracted using the E.Z.N.A.® DNA kit (Omega Bio-Tek, USA) for the CK, 3% OB, and 3% AB treatments. Subsequently, DNA purity and quality were assessed by a NanoDrop 2000 spectrophotometer (Thermo Scientific, USA), and the integrity was evaluated with 1% agarose gel. The primers 338F (5′-GTGCCAGCMGCCGCGG-3′) and 806R (5′-GGACTACHVGGGTWTCTAAT-3′) were selected for amplification of V3–V4 regions of the bacterial gene (Zhang M Y *et al*., 2020). The amplified polymerase chain reaction products were examined with 2% agarose gel and recovered by the AxyPrep DNA gel extraction kit (Axygen Biosciences, USA). High-throughput sequencing was conducted on the Illumina MiSeq platform (Illumina, USA) by Shanghai Majorbio Bio-Pharm Technology Co., Ltd., China.

Data processing and statistical analysis

Experimental data were shown as means ± standard deviations ($n = 4$). One-way analysis of variance (ANOVA) and Duncan's multi-interval test of SPSS software (V25.0) were used to test the significant differences among the treatments, and the difference was supposed to be significant at $P < 0.05$. Overall, the analysis of soil biological information was carried out at a branch of Shanghai Meiji Biomedical Technology Co., Ltd., China (http://www.isanger.com/index.html).

RESULTS

Biochar characterization

The SEM images showed a notable change in surface morphology of OB and AB; OB had a smoother surface than AB (Fig. 1a). After Al modification, AB surface became rougher, which might be due to the alterations in pore structure, pore size distribution, particle agglomeration, and surface coating. In addition, the SEM-EDS results indicated that the C content on AB surface decreased from 52.50% to 45.26% compared to that on OB surface, while the O, Mg, and Al contents increased by 6%, 72%, and 100%, respectively. Meanwhile, the elemental contents of K and Ca were reduced on AB surface. The FTIR spectra of OB and AB possessed similar characteristic peaks at 2 363, 1 596, 1 097, and 678 cm^{-1} (Fig. 1b). The absorbance peak at 2 363 cm^{-1} was probably the peak of CO_2, whereas the peaks at 1 596, 1 097, and 678 cm^{-1} were due to antisymmetric stretching and out-of-plane bending of aromatic C=O (ester), C–O (ether), and N–H (amide), respectively. Notably, an additional peak was observed in the case of AB at 3 398 and 652 cm^{-1}, which corresponded to –OH (phenolic) and Al–O (Al oxide), respectively. This change indicated that Al^{3+} ion became exchanged with other cations present in OB or adsorbed on biochar surface functional group, thus forming an Al complex on biochar surface. Therefore, AB had an additional functional group compared with OB. In addition, some peak intensities were reduced and shifted after Al modification. Moreover, the XRD analyses of OB and AB clearly indicated a great variation in crystallographic pattern (Fig. 1c). After Al modification, some peaks of $CaCO_3$ ($2\theta = 20.9°$, 29.2°, 39.3°, and 43.3°), $Ca(OH)_2$ ($2\theta = 28.1°$ and 49.96°), and SiO_2 ($2\theta = 26.7°$, 36.4°, and 50.1°) became reduced and disappeared for AB relatively to OB due to loading of Al oxide on the surface of AB.

Furthermore, the basic properties of OB and AB demonstrated that Al modification significantly reduced the pH of AB (4.24) as compared to OB (9.80), while increasing the ash contents by 8% relative to OB. The increase in ash content might be attributed to the inclusion of Al^{3+}, which formed the additional mineral component in the material. Additionally, in Al-modified biochar, the contents of water-soluble cations such as Ca^{2+} and Mg^{2+} increased by 80% and 62%, respectively, due to the alteration in biochar pH, which affected the solubility and mobility of Ca^{2+} and Mg^{2+}, potentially leading to higher water-soluble cation contents. Meanwhile, the Na^{+} content in AB was reduced by 88% because of the replacement of Na^{+} with Al^{3+} (Table SI, see Supplementary Material for Table SI). Thus, these improved properties of modified biochar were more conducive to the reclamation of saline-alkali soil.

Cation contents in soil leachates

To assess the contents of salts removed from the saline-alkali soil along with successive irrigations, we measured the chemical properties of soil leachates collected at different time intervals. Figure 2 displays the pH, EC, and water-soluble cation contents in the leachates of the saline-alkali soil. There were notable differences among the treatments. In the first leachate (*i.e*., on day 8), the pH and EC values were the highest, ranging from 8.30 to 8.91 and from 4.61 to 7.37 dS m^{-1}, respectively, across all treatments, which indicated that the maximum removal of salts from soil took place during the first irrigation. In the 3% OB and 3% AB treatments, the highest pH and EC values of soil leachate were recorded as compared to CK. In the subsequent leachate (*i.e*., on day 16), the pH and EC values were still higher; however, there was no significant difference in the pH and EC values of the third (*i.e*., on day 24) and fourth (*i.e*., on day 32) leachates between the 1% AB and 3% OB treatments. Notably, in the third and fourth leachates, the pH and EC

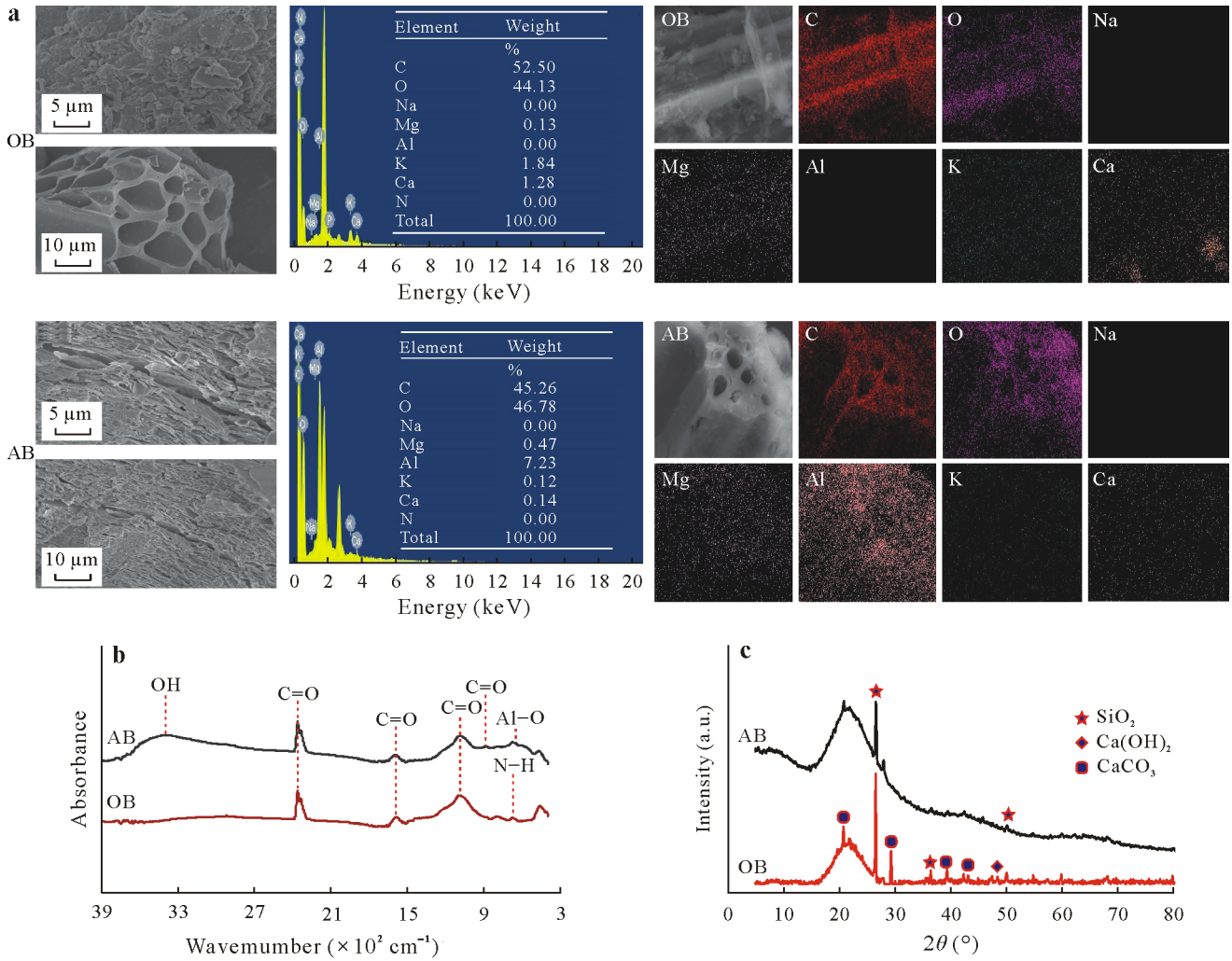

Fig. 1 Surface properties of biochar: scanning electron microscopy (SEM) images along with energy dispersive spectroscopy spectra (a), Fourier transform infrared spectra (b), and X-ray diffraction spectra (c) of original rice straw biochar (OB) and aluminum-modified rice straw biochar (AB). a.u. = arbitrary unit.

values in the 3% OB and 3% AB treatments were increased by 33%–41% and 66%–81%, respectively, relative to CK. Thus, the pH and EC values across four leachates fluctuated between 7.90 and 8.91 and between 0.60 and 7.37 dS m^{-1}, respectively.

The pH and EC values of soil leachates were highly correlated with the cation contents in soil solution. The contents of water-soluble cations such as Na^+, K^+, Ca^{2+}, and Mg^{2+} in soil leachate greatly varied among all treatments and decreased with an increase in number of irrigation (Fig. 2). In the first and second leachates, the content of water-soluble Na^+ varied from 1 245 to 2 650 mg L^{-1} and from 1 480 to 2 410 mg L^{-1}, respectively, whereas in the third and fourth leachates, the content of water-soluble Na^+ changed from 1 360 to 1 602 mg L^{-1} and from 851 to 1 016 mg L^{-1}, respectively. Notably, during the first and second leachates, the highest content of water-soluble Na^+ was observed in the 3% AB treatment, increased by 112% and 63%, respectively, relative to CK (Fig. 2). It was followed by the 3% OB treatment, increased by 77% and 45%, respectively, relative to CK. In the third soil leachate, there was no significant difference in the content of water-soluble Na^+ between the 3% AB and 3% OB treatments. While in the fourth soil leachate, the content of water-soluble Na^+ was lowered, particularly in the 3% AB treatment, which is evidence of the maximum removal of Na^+ taking place during the first irrigation. After successive irrigations, the average content of water-soluble Na^+ in soil leachate increased by 46.6% and 37.1%, respectively, in the 3% AB and 3% OB treatments relative to CK.

Meanwhile, the contents of water-soluble K^+, Ca^{2+}, and Mg^{2+} in soil leachates decreased with an increase in the number of irrigations and tended to become stable after the second irrigation. The contents of K^+ in the first, second, third, and fourth leachates increased by 37.9%–67.9%, 17.1%–42.5%, 17.4%–56.3%, and 18.2%–64.6%, respectively, in the respective biochar-amended treatments relative to CK (Fig. 2). Overall, the average contents of water-soluble K^+

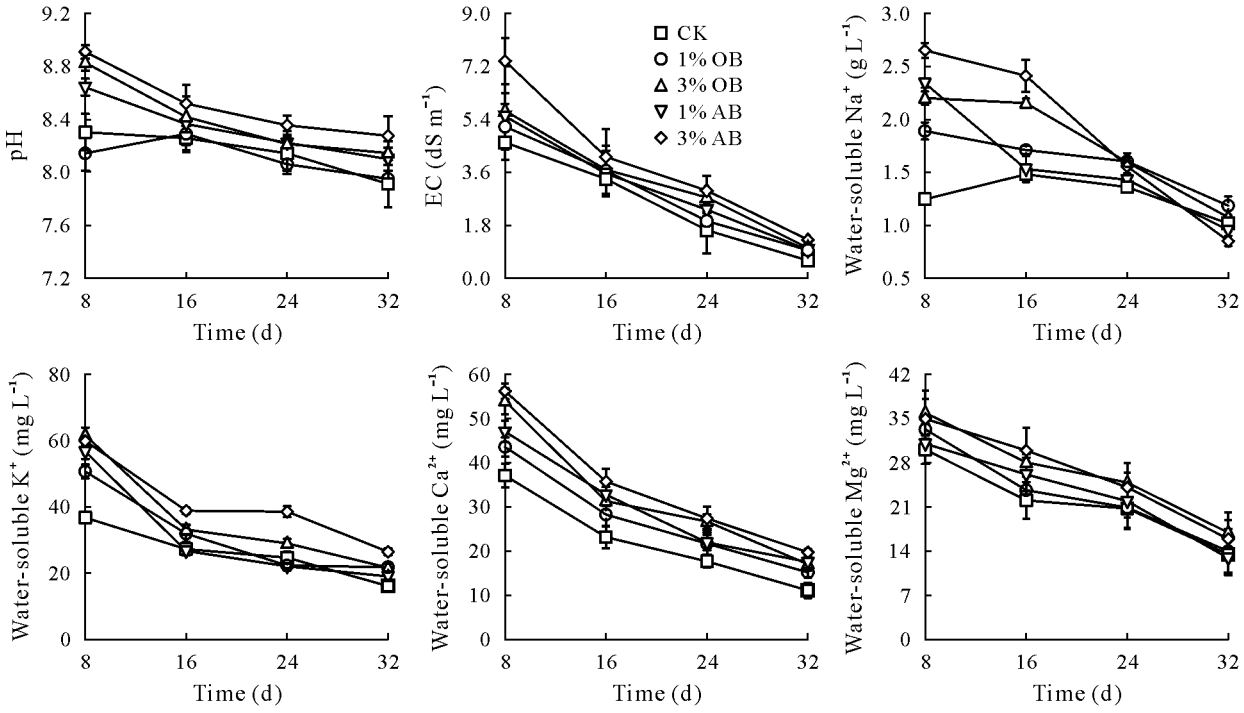

Fig. 2 Variations in pH, electrical conductivity (EC), and water-soluble cation contents in leachates of a saline-alkali soil collected on days 8, 16, 24, and 32 following irrigation practices in the treatments amended with 1% and 3% (weight:weight) original rice straw biochar (OB) and aluminum-modified rice straw biochar (AB) (1% OB, 3% OB, 1% AB, and 3% AB, respectively) and without biochar (control, CK). Vertical bars indicate standard deviations of the means ($n = 4$).

in the 3% OB and 3% AB treatments increased by 40.0% and 56.3%, respectively, relative to CK, whereas the average contents of Ca^{2+} and Mg^{2+} in the biochar-amended treatments increased by 22.7%–55.2% and 7.8%–21.5%, respectively, compared to CK (Fig. 2). The highest contents of Ca^{2+} and Mg^{2+} were reported in the first and second leachates, while the lowest contents were in the third and fourth leachates. However, there was no significant difference in the Ca^{2+} and Mg^{2+} contents between the 3% AB and 3% OB treatments. In short, a decreasing trend in the contents of water-soluble cations was observed after four successive irrigations, and as a result, salinity stress in the saline-alkali soil was greatly reduced.

Soil physicochemical properties

In order to enumerate the effects of biochar addition and irrigation practices on the reclamation of saline-alkali soil, we analyzed the physicochemical properties of the saline-alkali soil. The 3% AB treatment showed a more noticeable impact on the improvement of soil properties after four successive irrigations, decreasing soil pH, EC, and SAR by 7.8%, 27.4%, and 36.77%, respectively, relative to CK (Fig. 3). In contrast, SOM increased by 7.71 folds in the 3% AB treatment as compared to CK (Fig. 3).

Furthermore, the contents of water-soluble cations Na^+, K^+, Ca^{2+}, and Mg^{2+} in the saline-alkali soil after four successive irrigations were significantly influenced by the biochar-amended treatments (Fig. 4). The water-soluble Na^+ content in biochar-amended soils was dramatically reduced by 4.8%–28.2%, whereas the K^+ content increased by 20.18%–55.29%. The highest reduction rate of water-soluble Na^+ content was reported in the 3% AB treatment. In addition, the water-soluble Ca^{2+} and Mg^{2+} contents increased by 13.8%–31.8% and 20.6%–59.6%, respectively, in the biochar-amended treatments relative to CK. Additionally, the variations in water-soluble cations were closely linked to the alterations in the pool of exchangeable cations in soil. The contents of exchangeable cations greatly varied among different treatments (Fig. 4). After biomass application, the content of exchangeable Na^+ was reduced by 11.7%–30.2% compared to CK. However, there was no significant difference in the content of exchangeable Na^+ between CK and 1% OB treatment (Fig. 4). In addition, exchangeable K^+ increased by 12.8%–45.5%; the highest content of exchangeable K^+ was reported in the 3% OB treatment (Fig. 4). Meanwhile, the contents of exchangeable Ca^{2+} and Mg^{2+} were improved by 12.4%–35.9% and 25.5%–60.4%, respectively, after biochar application compared to CK (Fig. 4).

Overall, biochar application, particularly modified biochar addition, greatly improved soil physicochemical properties by reducing the Na^+ content as well as increasing the K^+, Ca^{2+}, and Mg^{2+} contents, due to its high affinity for Na^+ displacement and gradual release of bound nutrients from biochar. These improvements in soil properties led to

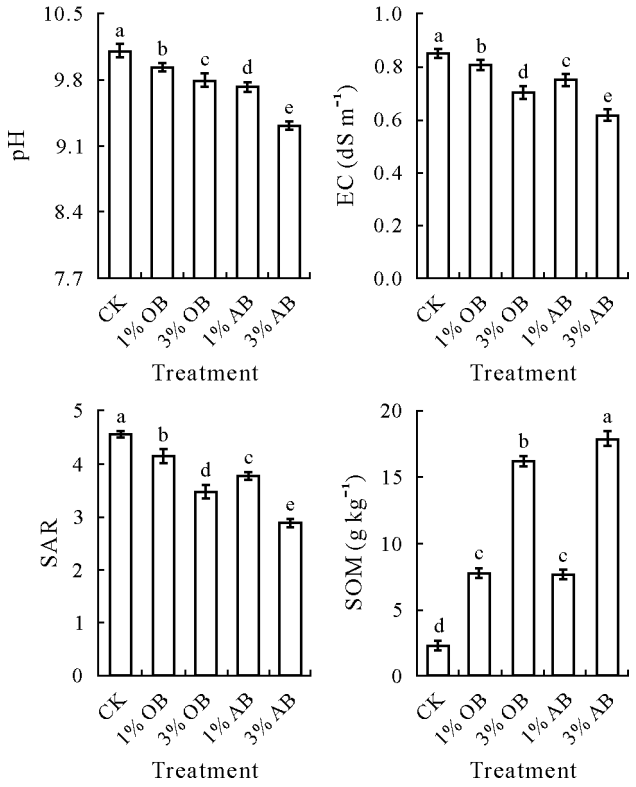

Fig. 3 Variations in pH, electrical conductivity (EC), sodium adsorption ratio (SAR), and organic matter (SOM) of a saline-alkali soil after four successive irrigations in the treatments amended with 1% and 3% (weight:weight) original rice straw biochar (OB) and aluminum-modified rice straw biochar (AB) (1% OB, 3% OB, 1% AB, and 3% AB, respectively) and without biochar (control, CK). Vertical bars indicate standard deviations of the means ($n = 4$). Different letters indicate significant differences at $P < 0.05$ according to Duncan's test.

the augmentation of soil extracellular enzyme activities and fostered soil microbial community.

Soil extracellular enzyme activities

Soil extracellular enzyme activity is a crucial indicator for determining soil microbial processes, nutrient cycling, organic matter decomposition, and overall soil health. In our study, the activities of C cycling-related enzymes such as β-1,4-glucosidase (βG) and β-cellobiohydrolase (CBH) were significantly improved among the biochar-amended treatments compared to CK (Fig. 5). However, there was no significant difference in βG activity between the OB and AB treatments. Notably, in the 3% AB treatment, the βG and CBH activities increased by 1.14 and 1.93 folds, respectively, relative to CK. Additionally, the highest β-1,4-*N*-acetylglucosaminidase (NAG) activity was reported in the 1% OB treatment (Fig. 5). Such variations in enzyme activity affected bacterial composition by altering nutrient availability and substrate utilization.

Moreover, the results of two-factor redundancy analysis (RDA) between soil microbial community and enzyme activity showed that the first (RDA1) and second (RDA2) axes accounted for 41.92% of the variation in bacterial composition at species level, of which RDA1 accounted for 34.12% and RDA2 accounted for 7.80% (Fig. S1, see Supplementary Material for Fig. S1). Notably, the application of AB and OB positively influenced the CBH and βG activities, which were closely associated with cellulose degradation and nutrient cycling.

Soil microbial properties

The results of high-throughput sequencing unambiguously presented that bacterial composition greatly varied among all treatments. Overall, 54 977 sequences were acquired from 12 soil samples. The differences at operational taxonomic unit (OTU) level with biochar application were illustrated by the scatter plot of principal component analysis, showing a clear degree of separation in microbial community structure among CK, 3% OB, and 3% AB treatments (Fig. 6a). In addition, the alpha diversity test of inter-group differences at OTU level showed that Shannon index exhibited a significant difference ($P < 0.05$) between CK and biochar-amended treatments (*i.e.*, 3% OB and 3% AB treatments) (Fig. 6b). The index Sobs greatly varied between CK and 3% OB treatment (Fig. 6c). Meanwhile, there was no significant difference in Chao 1 among all treatments (Fig. 6d).

Moreover, the results of two-factor RDA between soil microbial community and exchangeable cations showed that RDA1 and RDA2 accounted for 57.95% of the total variation in soil microbial community, with 37.32% explained by RDA1 and 20.63% by RDA2. It was indicated that exchangeable cations such as Ca^{2+}, Mg^{2+}, and K^{+} induced by AB and OB application were strongly associated with soil microbial community (Fig. S2, see Supplementary Material for Fig. S2). Among soil microbial community structure, Proteobacteria, Actinobacteriota, Firmicutes, Chloroflexi, Gemmatimonadota, and Bacteroidota were common bacterial phyla in the biochar-amended and non-amended saline-alkali soils (Fig. 6e). However, the relative abundances of Proteobacteria and Actinobacteriota in the 3% AB treatment were higher than those in CK and 3% OB treatment, whereas the relative abundance of Bacteroidota was lower. At the genus level, a noticeable difference in soil bacterial composition was also observed. *Bacillus*, norank_f_JG30-KF-CM45, norank_f_Longimicrobiaceae, norank_f_Euzebyacceae, and norank_f_Nitriliruptoraceae were dominant bacteria at the genus level (Fig. 6f). In the 3% AB treatment, the relative abundances of norank_f_JG30-KF-CM45, norank_f_Longimicrobiaceae, and norank_f_Euzebyacceae were increased by 21%, 9%, and 18%, respectively, whereas the abundance of *Bacillus* decreased by 21% in comparison to the 3% OB treatment. Meanwhile, *Pontibacter*, a phosphate-solubilizing bacterium, had the highest relative abundance in the 3% OB treatment.

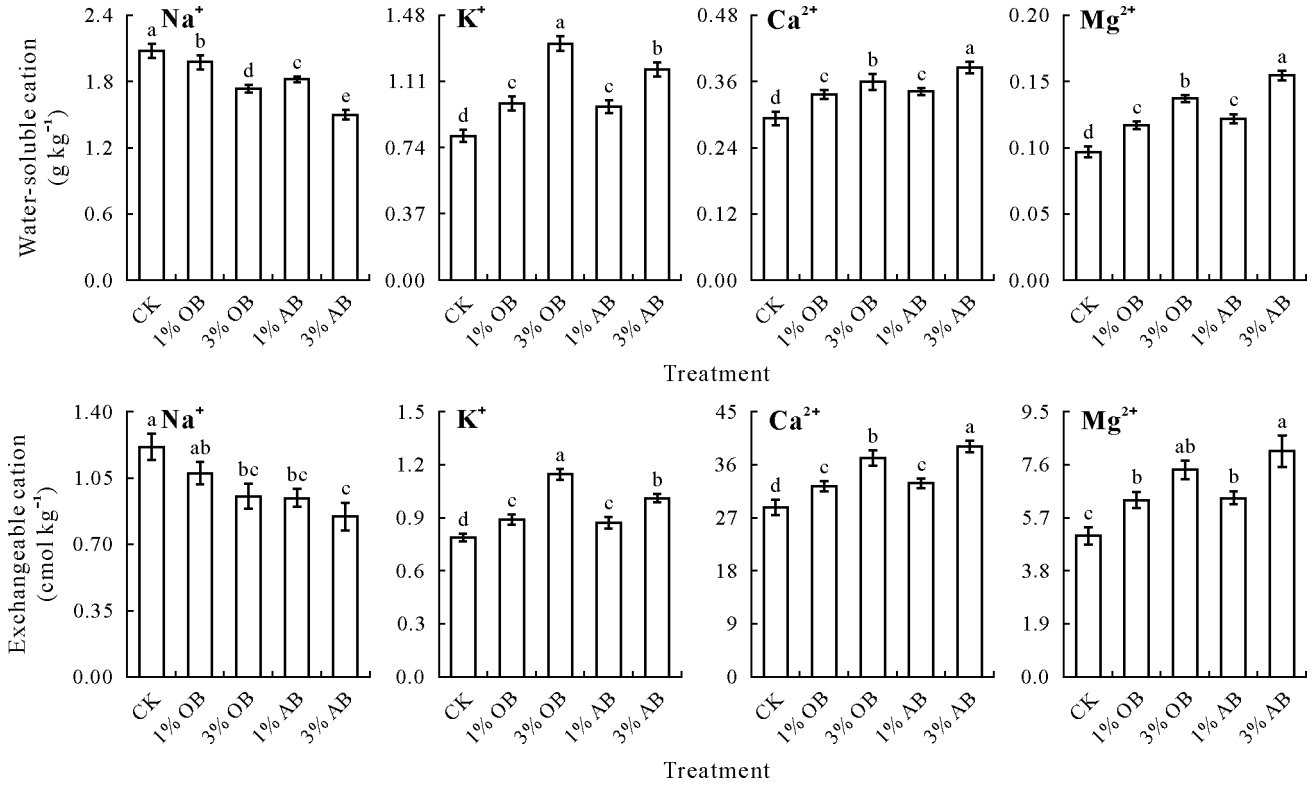

Fig. 4 Contents of water-soluble and exchangeable cations in a saline-alkali soil after four successive irrigations in the treatments amended with 1% and 3% (weight:weight) original rice straw biochar (OB) and aluminum-modified rice straw biochar (AB) (1% OB, 3% OB, 1% AB, and 3% AB, respectively) and without biochar (control, CK). Vertical bars indicate standard deviations of the means ($n = 4$). Different letters indicate significant differences at $P < 0.05$ according to Duncan's test.

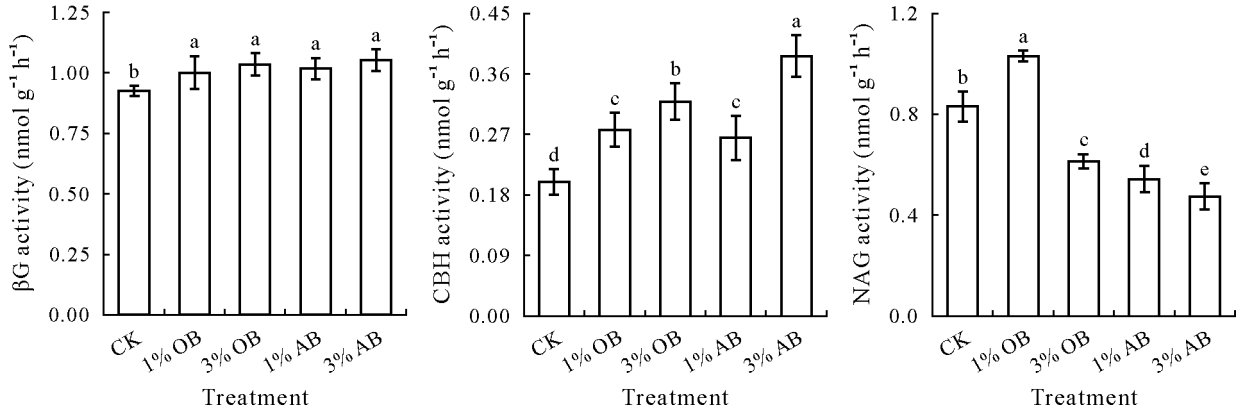

Fig. 5 Activities of extracellular enzymes, C cycling-related β-1,4-glucosidase (βG) and β-cellobiohydrolase (CBH) and N cycling-related β-1,4-*N*-acetylglucosaminidase (NAG), of a saline-alkali soil after four successive irrigations in the treatments amended with 1% and 3% (weight:weight) original rice straw biochar (OB) and aluminum-modified rice straw biochar (AB) (1% OB, 3% OB, 1% AB, and 3% AB, respectively) and without biochar (control, CK). Vertical bars indicate standard deviations of the means ($n = 4$). Different letters indicate significant differences at $P < 0.05$ according to Duncan's test.

Interestingly, in order to elucidate which microorganisms showed statistically substantial variations, two groups of soil microbial community at the genus level between CK and 3% AB treatment and between 3% OB and 3% AB treatments were compared to determine differential microorganisms in the 3% AB treatment (Fig. 7). The results showed that in the 3% AB treatment, the relative abundances of norank_f_Longimicrobiaceae, norank_c_Alphaproteobacteria, *Sphingomonas*, and *Nitrosococcus* were the highest, while the relative abundances of norank_f_JG30-KF-CM4, norank_f_Nitriliruptoraceae, norank_c_BD2-11_terrestrial_group, and unclassified_f_Cyclobacteriaceae were lowered compared to CK.

Furthermore, 3% AB addition induced a prominent increment in the relative abundances of norank_f_Symbiobacteraceae, norank_c_Alphaproteobacteria, *Sphingomonas*, and unclassified_c_Actinobacteria, while decreasing the relative abundances of *Bacillus*, *Pontibacter*, and unclassified_

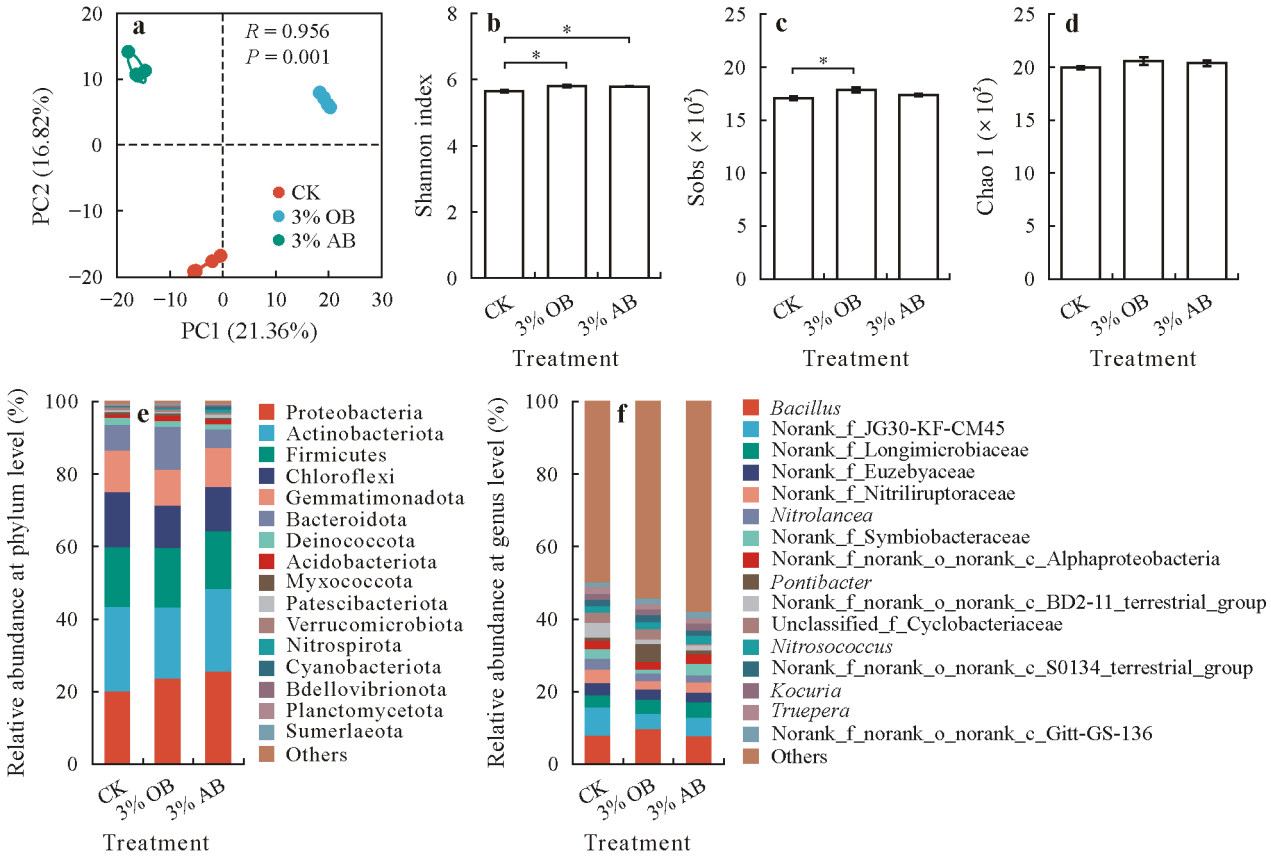

Fig. 6 Principal component (PC) analysis (a) and alpha diversity, shown as Shannon index (b), Sobs (c), and Chao 1 (d), at operational taxonomic unit level and relative abundances at phylum (e) and genus (f) levels of microbial community of a saline-alkali soil after four successive irrigations in the treatments amended with 3% (weight:weight) original rice straw biochar (OB) and aluminum-modified rice straw biochar (AB) (3% OB and 3% AB, respectively) and without biochar (control, CK). In panels b, c, and d, vertical bars indicate standard deviations of the means ($n = 4$). Asterisk * indicates significant differences at $P < 0.05$.

f_Cyclobacteriaceae as compared to 3% OB addition. These changes in soil microbial community were further elaborated *via* the linear discriminant biomarker analysis (LEfSe), showing that 48 microbial biomarkers existed in the 3% AB treatment, which was lower than the 3% OB treatment (Fig. S3, see Supplementary Material for Fig. S3). The most dominant class in the 3% AB treatment was Alphaproteobacteria, phylum Proteobacteria, orders Rhizobiales, Sphingomonadales, and Burkholdaleriales, and family Sphongomonodaceae, whereas in the 3% OB treatment, the dominant class was Bacteriodia, phylum Bacteriodota, and family Bacillaceae.

A single-factor correlation network between microbial species indicated that the number of nodes and edges increased after OB and AB application compared to CK (Fig. S4, see Supplementary Material for Fig. S4). In the AB treatment, the total numbers of nodes and edges were 62 and 133, respectively, whereas in the OB treatment, 54 nodes and 139 edges were formed. In contrast, the network analysis showed 42 nodes and 137 edges in CK. These results indicate that biochar application modified the interaction between bacterial species. Interestingly, the heatmap analysis showed that soil bacterial community structure was significantly influenced by soil properties both at the phylum and genus levels. Soil pH, EC, SAR, exchangeable Na^+, and NAG activity showed strong positive correlations with the relative abundances of Planctomycetota and Desulfobacterota, whereas robust negative correlations with the relative abundances of Nitrospirota and Cynobacteriota at the phylum level (Fig. 8a). Meanwhile, SOM and other exchangeable cations such as K^+, Ca^{2+}, and Mg^{2+} were positively linked to the relative abundances of Nitrospirota, Cynobacteriota, and Proteobacteria. Additionally, the CBH and βG activities also enhanced the relative abundances of these groups. Whereas, at the genus level, soil pH, EC, SAR, and NAG activity were positively associated with the relative abundances of unclassified_f_Cyclobacteriaceae and *Halomas* and negatively correlated with the relative abundances of norank_f_Longimicrobiaceae and norank_c_Alphaproteobacteria (Fig. 8b).

Additionally, the results of the interactive Mantel test analysis between microbial communities and soil nutrients, as well as extracellular enzyme activities, indicated that the alpha diversity index and bacterial composition altered with the variation in soil chemical properties (Fig. S5, see

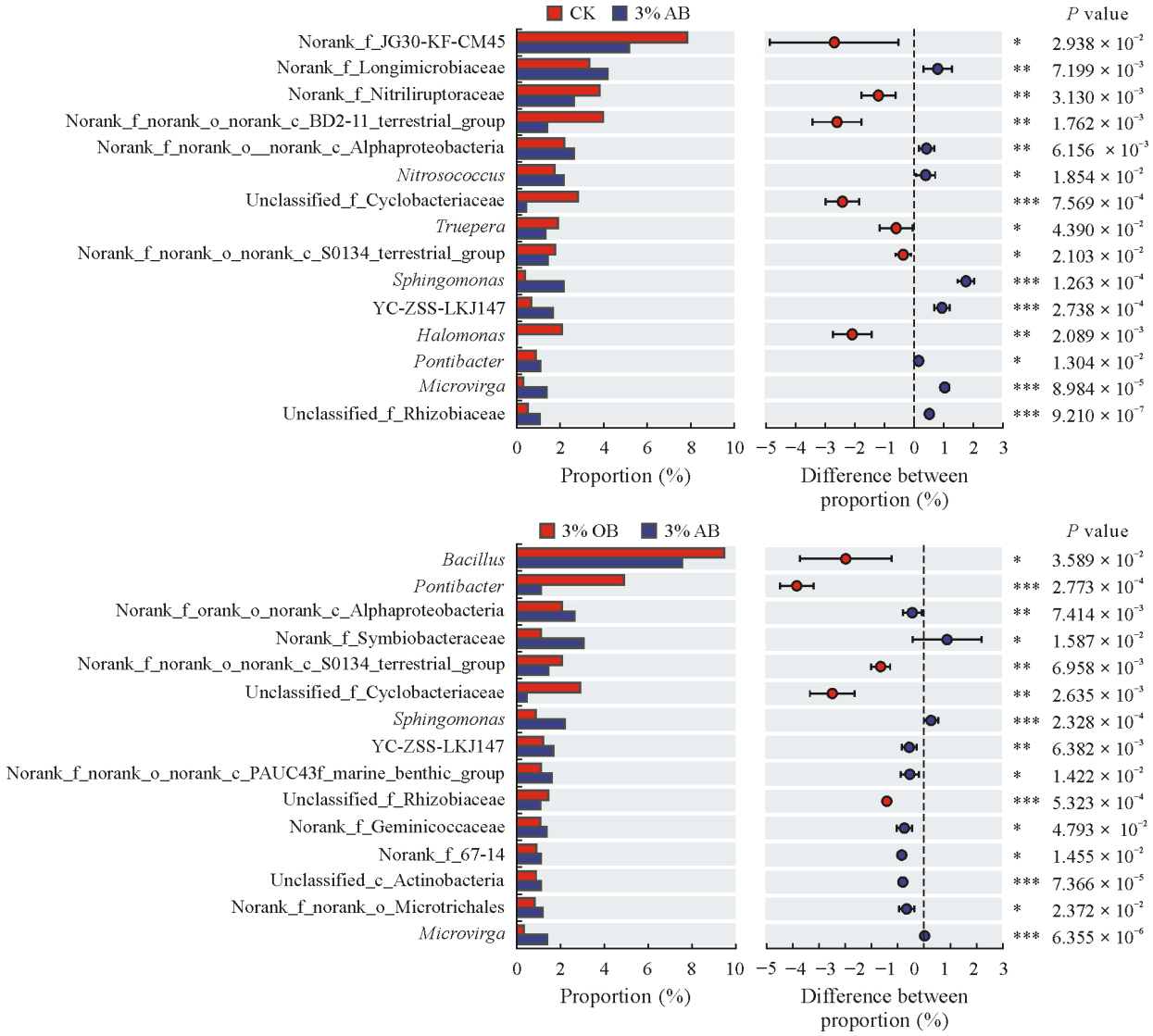

Fig. 7 Comparisons of two groups of microbial community at genus level of a saline-alkali soil between the treatments amended with 3% (weight:weight) original rice straw biochar (OB) and aluminum-modified rice straw biochar (AB) (3% OB and 3% AB, respectively) and without biochar (control, CK). Horizontal bars indicate 95% confidence intervals. Asterisks *, **, and *** indicate significant differences at $P < 0.05$, $P < 0.01$, and $P < 0.001$, respectively.

Supplementary Material for Fig. S5). Notably, the alpha diversity index showed negative correlations with exchangeable cations except Mg^{2+}. Thus, an obvious change in bacterial structure was encountered with the alteration in soil properties.

DISCUSSION

Effects of biochar application on soil leachate pH, EC, and cation contents

Biochar application with irrigation practices significantly altered pH, EC, and water-soluble cation contents in soil leachate at different time intervals, showing a decreasing trend among all treatments (Fig. 2). During the first irrigation, the pH and EC values of the leachates were higher due to the maximum removal of salts, particularly Na^+ replaced from the soil matrix. Among all treatments, the 3% AB treatment was more effective in lowering the salt content. High content of Al in AB replaces more Na^+ and other cations from the soil exchange sites and, in turn, increases their contents in leachate (Huang *et al*., 2023). The decreasing trend in pH and EC values of leachates was in line with the findings of Xu *et al*. (2023). After the third irrigation, the contents of Na^+, K^+, Ca^{2+}, and Mg^{2+} in leachate tended to become stable, but were still significantly higher in the 3% AB treatment as compared to other treatments. The possible reason is that Al modification further enhances the CEC of biochar and induced competition for exchange sites; as a result, more cations are displaced from the soil matrix upon Al-modified biochar application (Zheng *et al*., 2020).

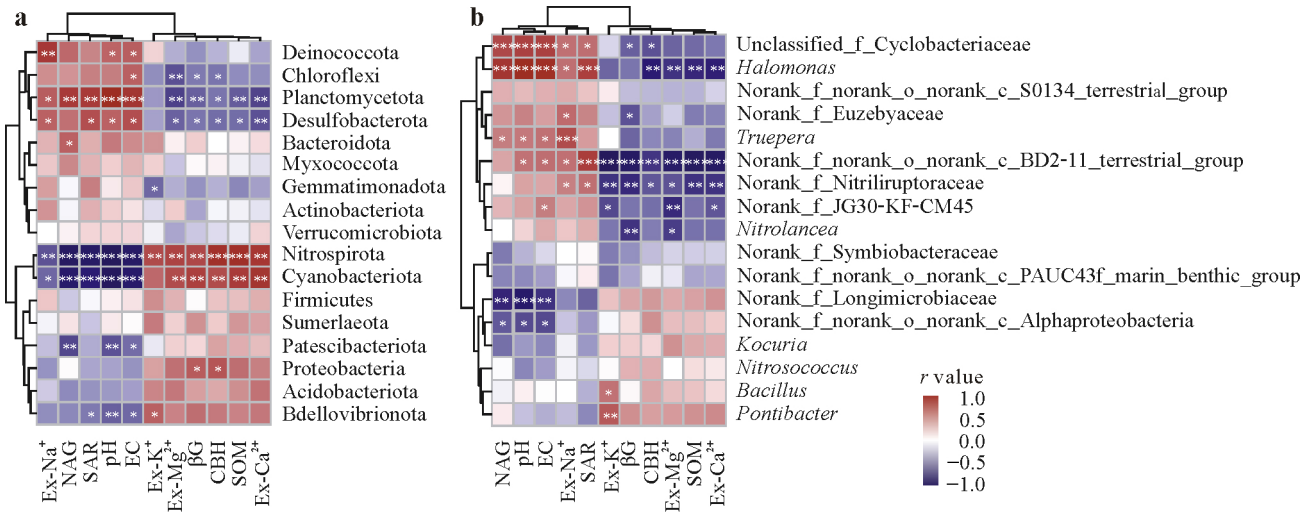

Fig. 8 Heatmaps showing Spearman correlation analysis between relative richness ($n = 4$) of the top 17 microbial species and physicochemical properties and enzyme activities at phylum (a) and genus (b) levels of a saline-alkali soil. Asterisks *, **, and *** indicate significant correlations at $P < 0.05$, $P < 0.01$, and $P < 0.001$, respectively. EC = electrical conductivity; SAR = sodium adsorption ratio; SOM = soil organic matter; Ex-Na^+, Ex-K^+, Ex-Mg^{2+}, and Ex-Ca^{2+} = exchangeable Na^+, K^+, Mg^{2+}, and Ca^{2+}, respectively; NAG = β-1,4-*N*-acetylglucosaminidase; βG = β-1,4-glucosidase; CBH = β-cellobiohydrolase.

In general, great ion exchange, particularly between Al^{3+} and Na^+, occurs primarily due to the differences in their ionic charge density or size. Al^{3+}, being a trivalent ion, has a higher charge density (+3) than monovalent Na^+ (+1). This higher charge density creates a stronger electrostatic attraction for negatively charged sites within the soil matrix or exchange sites. Thus, when Al-modified biochar is added to Na^+-enriched saline-alkali soil, it competes for the exchange sites (Li *et al*., 2022; Singh *et al*., 2023). Due to its higher charge density, Al^{3+} preferentially displaces Na^+ from the exchange sites and releases Na^+ in soil solution. Such an ion exchange process mainly works on the principle of electrostatic equilibrium, where the ions with higher charge density have a greater affinity for the negatively charged surfaces and replace the ions with lower charge density (Peng C *et al*., 2023). Additionally, the smaller ionic radius of Al^{3+} compared to Na^+ further enhances its ability to fit into the exchange sites efficiently, reinforcing the displacement process (Ouhadi and Goodarzi, 2006; Zhou *et al*., 2019).

Furthermore, a complex interaction between Al^{3+} ions and biochar surface functional groups, such as carboxyl and hydroxyl groups, has influenced the selectivity for specific cations, leading to the preferential release of Na^+, K^+, Ca^{2+}, and Mg^{2+} into leachate. Such selectivity for specific cations depends on the structure and stability of the Al-carboxyl complex, cation size, and charge density, as well as hydration energy and affinity of cations for surface functional groups (Mandal *et al*., 2021). In addition, the pH, surface properties, and feedstock composition of biochar also affect the sorption and desorption of cations from the soil matrix (Wang K *et al*., 2024; Wang X L *et al*., 2024b). Our result demonstrated that with an increase in the number of irrigations, the contents of water-soluble cations in soil leachate became reduced (Zhang Y *et al*., 2020; Xu *et al*., 2023). In the fourth leachate, the contents of water-soluble cations were lowered as compared to the other leachates. However, the contents of K^+, Ca^{2+}, and Mg^{2+} in leachate in the 3% AB treatment were a little higher compared to the other treatments, due to the slow release of cations from biochar over an extended period (Li *et al*., 2022). In addition, the application of Al-modified biochar effectively lowers soil pH and enhances the solubility of certain minerals and nutrients; as a result, more K^+, Ca^{2+}, and Mg^{2+} can be released (Hameed *et al*., 2024). Notably, AB addition improves soil structure, which increases water retention and aeration. Such improvements in soil physical properties with modified biochar application can further accelerate the nutrient mobilization and availability (Lin *et al*., 2024; Wang *et al*., 2025). However, it is well understood from these findings that only limited irrigation can drain off the water-soluble cations and can lower the salt contents in the soil. Excessive irrigation practices not only cause water losses, but also remove the essential cations from the soil, which are important for plant growth and development.

Alterations in soil physiochemical properties after biochar application and successive irrigations

Biochar application and irrigation practices greatly affected soil physiochemical properties and induced a positive impact by lowering the salt contents in saline-alkali soil. Reduction in salt contents with biochar application is attributed to an improved soil structure that facilitates better water infiltration and percolation, as well as to pH regulation that enhances salt mobility for effective leaching (Yin *et al*., 2022). Among all treatments, soil pH, EC, and SAR were

greatly reduced, particularly in the 3% AB treatment (Fig. 3). This is due to the acidic nature of AB, which is altered with the introduction of Al^{3+}, neutralizing alkaline salts and promoting salt leaching (Yin *et al*., 2018; Peng C *et al*., 2023). Moreover, Wang Y P *et al*. (2024) stated that the biochar with low pH had a high adsorption capacity due to a large number of O-containing functional groups, while the biochar with high pH had a low adsorption capacity because of competition for hydroxyl ions on the biochar surface. Additionally, Al modification promotes the formation of organo-mineral complexes and enhances ion exchange reaction, which also modifies soil ionic balance (Qian and Chen, 2014).

Our findings were in line with the study of Phuong Tran *et al*. (2021), who reported that the reductions in EC and SAR values of saline-alkali soil were mainly due to the high affinity of Al^{3+} ions to displace Na^{+} ions by forming complexes or competing with Na^{+} for binding sites on biochar surfaces. Additionally, high CEC and surface positive charge density of modified biochar alter the nutrient status in soil by lowering Na content (Gao *et al*., 2024). All these mechanisms collectively reduced soil pH, EC, and SAR. Meanwhile, AB addition greatly improved the SOM content, which is an important indicator of soil fertility (Fig. 3). The reason behind this increase is that during biochar modification, additional functional groups were created on the biochar surface; as a result, the surface chemistry of biochar became altered, which may enhance microbial decomposition of organic residues and C sequestration (Deng *et al*., 2021; Huang *et al*., 2023). In addition, the interaction of Al^{3+} ions and organic C encouraged the formation of stable organo-metal complexes that further enhanced organic matter accumulation. Such an increase in SOM contributes to the long-term process involved in the improvement of soil fertility (Porras *et al*., 2017; Patrick *et al*., 2022).

Variations in soil pH, EC, and SOM resulting from biochar application significantly correlate with the water-soluble and exchangeable cations in soil (Gao *et al*., 2024). High contents of water-soluble and exchangeable cations, particularly Na^{+}, induce soil compaction, hindering salt leaching, root penetration, and plant growth (Saifullah *et al*., 2018; Du *et al*., 2023). In such conditions, biochar application plays a key role in improving the properties of saline-alkali soil by increasing soil CEC, porosity, and hydraulic conductivity, which facilitate the salt leaching by irrigation water and promote the retention of essential nutrients through the large surface area of biochar (Liang *et al*., 2021; Adhikari *et al*., 2024). Thus, in our study, AB showed a better effect in reducing the Na^{+} content as compared to OB, due to its larger surface area and higher adsorption capacity after Al modification, which led to greater salt adsorption on its surface or into its pores, where they are displaced with time (Zhang *et al*., 2021).

In a previous study, He *et al*. (2020) identified two basic mechanisms, by which the Al-modified biochar induces a considerable change in surface charge density and, in turn, helps in reducing salt content in saline-alkali soils. Firstly, Al^{3+} ions form metal complexes with functional groups present in biochar; as a result, negatively charged sites of biochar become reduced, while the surface positive charge density simultaneously increases (Qian and Chen, 2014). This alteration in surface charge density makes the biochar more suitable for retaining essential nutrients while repelling excess Na^{+} ions associated with salt stress (Gao *et al*., 2024). Secondly, the physical covering of Al oxide on the functional groups of biochar further decreases the negative charge on its surface. This physical barrier decreases the repulsion of negatively charged ions, substantially boosting the biochar's ability to interact with or immobilize the Na^{+} ions inside the soil matrix (Li *et al*., 2022). Collectively, these variations in surface charge density generated by Al modification make the biochar more proficient in lowering Na^{+} content in saline-alkali soils, hence contributing to the improvement of soil health. The above statement supports our results that the 3% AB treatment showed a better effect in reducing the salt content in the saline-alkali soil than other treatments.

Moreover, biochar application further improved soil properties by increasing the contents of multivalent cations such as K^{+}, Ca^{2+}, and Mg^{2+}. These cations further reduced the Na^{+} ions by forming cation bridges between soil minerals and biochar (Adhikari *et al*., 2024). The bridge structure facilitates the oxidation of C–C, C=C, and C–H into C–O, C=O, and –COOH on biochar surface and induces acidic functional groups on biochar surface that promote the formation of mineral complexes (Yang *et al*., 2021). Among acidic functional groups, the carboxylic (–COOH) and phenolic (–OH) groups possess a strong affinity to form a complex with Na^{+} ions and thus enhance the leaching of Na^{+} ions through irrigation (Siedt *et al*., 2021; Singh *et al*., 2023). Additionally, Ca^{2+} ions in soil usually act as coagulating agents and possess a strong affinity to displace Na^{+} ions from the soil exchange sites (Saifullah *et al*., 2018), in turn promoting soil aggregation, aeration, water infiltration, and nutrient availability (Lee *et al*., 2022).

Interestingly, the K content in the 3% AB-treated soil was lower than that in the 3% OB-treated soil, possibly due to the complex interaction between Al^{3+} and K^{+} ions. In addition, during biochar modification with Al, ion exchange and immobilization phenomena occur (Peng C *et al*., 2023; Peng Y T *et al*., 2023) that lead to displacing K^{+} on biochar surface with Al^{3+}; as a result, insoluble compounds or precipitates form, which reduces K availability in soil (Gao *et al*., 2024). While the Mg^{2+} content in the 3% AB treatment was the highest, which could be attributed to the greater Mg^{2+} content in AB due to the formation of Al-Mg complex and retained Mg^{2+} ions on biochar surface (Zheng *et al*.,

2020). Moreover, the aggregation or precipitation of Mg^{2+} on biochar surface after Al modification could be another reason for the higher Mg^{2+} content found in the AB-treated saline-alkali soil (Wu *et al*., 2019). Concisely, AB application greatly reduced the salt content in the saline-alkali soil by the mechanisms of ion exchange, dilution effect, adsorption, and precipitation.

Alterations in soil extracellular enzyme activities and microbial community structure after biochar application and successive irrigations

Extracellular enzymes are essential for the biogeochemical cycling of nutrients, especially for C, nitrogen, and phosphorus, in turn affecting soil ecosystem functioning (Liu *et al*., 2024). High salt content and high pH of saline-alkali soil alter soil edaphic environment, causing ion toxicity and osmotic stress, both of which retard soil enzyme activities (Zhang *et al*., 2024). Under salt stress, biochar application in saline-alkali soils not only reduces the salt content, but also promotes the enzyme activities (Peng Y T *et al*., 2023). In our study, a significant improvement in βG and CBH activities was observed under biochar application (Fig. 5), which might be due to the complex interaction between soil pH, organic matter, nutrient availability, and ion content (Wang K *et al*., 2024). In addition, high SOM content, particularly in the AB treatment, greatly enhanced the βG and CBH activities (Rahmanian and Khadem, 2024; Wang X L *et al*., 2024a). In contrast, a decline in the NAG activity in the AB-amended soil (Fig. 5) may be attributed to the high N content, which could potentially slow down the mineralization rate of organic N and lead to a reduction in the NAG activity (Gaudel *et al*., 2024). Overall, these results are aligned with the findings of Zhang C *et al*. (2023) and Zhang N H *et al*. (2023), who reported that biochar application increased SOM and microbial biomass C, which in turn improved the extracellular enzyme activities. Additionally, biochar application provides a suitable environment that further promotes soil enzyme activities through its unique properties, such as high porosity, large surface area, and active adsorption sites, which help in lowering the ion toxicity either by leaching or adsorbing the ions (Pandey *et al*., 2020; Peng Y T *et al*., 2023).

In addition, biochar application also positively influences soil microbial community structure (Yin *et al*., 2022), which is one of the important biological indicators of soil ecosystem functioning (Cui *et al*., 2023). In the current study, soil microbial community was greatly influenced by biochar application, as evidenced by the distinct differences observed in Fig. 6a–d. Biochar addition in saline-alkali soils induces a prominent impact on soil properties by lowering the salt content *via* leaching or adsorption and provides a suitable microhabitat for microbial growth (Chen *et al*., 2017). In addition, the alteration in soil nutrient status with biochar application also affects the diversity and composition of soil microbial communities (Gao *et al*., 2024). Our results reported notable variations in soil microbial diversity and richness among all treatments, which are aligned with the above statements. Proteobacteria, Actinobacteriota, Firmicutes, and Chloroflexi were dominant phyla, whereas at the genus level, *Bacillus* and norank f_JG30-KF-CM45 were the top genera regarding their richness among the different treatments (Fig. 6e, f). The relative abundances of Proteobacteria and Actinobacteriota were higher in the 3% AB treatment as compared to the other treatments. These findings are quite similar to the study of Zhang *et al*. (2022), who found that biochar application in saline-alkali soils significantly improved the relative abundance of Proteobacteria, whereas reduced the relative abundance of Bacteroidetes, by altering soil chemical properties, such as lowering pH, exchangeable sodium percentage, and EC and increasing organic matter and nutrient availability.

Furthermore, Proteobacteria, Actinobacteriota, Firmicutes, and Chloroflexi possess a strong salt tolerance mechanism and robust structural adaptation toward soil salinity; that's the reason why they are abundant in saline-alkali soils and beneficial for soil health (Wang X L *et al*., 2024a). Proteobacteria (Gram-negative) are copiotrophic bacteria that prefer a nutrient-rich environment for their survival, are involved in organic matter decomposition and nutrient cycling, particularly in N cycling, and can reduce N losses (Zhang S X *et al*., 2023). Actinobacteriota (Gram-negative bacteria) are involved in the degradation of organic pollutants and provide resistance against pathogens (Sharma *et al*., 2023). Both Proteobacteria and Actinobacteriota are also involved in phytohormone release, siderophore production, osmoregulation, and exopolysaccharide secretion that further improve soil structure and promote the soil-plant-microbe interaction (Ebrahimi-Zarandi *et al*., 2023). Firmicutes, Gram-positive bacteria, possess a ubiquitous presence and versatile adaptability in saline-alkali soils and can release various plant growth-promoting substances that improve root growth and nutrient uptake. Additionally, they are involved in anaerobic degradation of cellulosic substances and showed positive correlations with SOM and basic cations (Cui *et al*., 2023). Chloroflexi, photoautotrophic bacteria, play an essential role in carbohydrate metabolism (Ablimit *et al*., 2022) and indicate negative correlations with SOM and exchangeable cations except for Na^+ (Fig. 8). These findings are consistent with Ramírez *et al*. (2020), who found that the richness of Chloroflexi was negatively correlated with soil organic C fraction. Thus, the variations in soil organic C fractions or organic C content in soil aggregates are closely associated with bacterial abundance.

At the genus level, a significant improvement in beneficial plant growth-promoting rhizobacteria such as norank_f_JG30-KF-CM45, norank_f_Symbiobacteraceae, and

Sphingomonas was encountered (Fig. 7). These bacteria are usually involved in nutrient cycling, organic decomposition, and heavy metal phytoremediation (Lin *et al*., 2021), as well as enhanced plant resistance against disease (Sharma *et al*., 2023). According to Wang X L *et al*. (2024b), the variations in soil bacterial communities arise from the changes in soil environment, and the diversity of bacterial community declines as salinity stress increases. High salt stress induces a great restriction in colonization and expansion of bacterial populations (Cao *et al*., 2023; Feng *et al*., 2023). Additionally, soil enzyme activities are also closely associated with soil bacterial community composition (Li *et al*., 2019).

Overall, AB exhibited a strong potential to reclaim the saline-alkali soil by lowering the Na^+ content, improving soil structure, and modifying soil microbial community structure and functionalities that can facilitate a healthier soil environment for plant growth. The AB could be beneficial only when applied in conjunction with effective irrigation practices. Regular irrigation practices not only reduce the Na^+ content, but also facilitate the leaching of excessive Al^{3+} ions, thereby minimizing the risk of Al toxicity over time. This synergy will enhance soil quality and support sustainable agricultural practices. In the future, further research is needed to explore the long-term impacts of AB application on saline-alkali soils in depth by monitoring Al^{3+} content and evaluating its effects on soil health and ecosystem functioning.

CONCLUSIONS

In this study, the application of AB along with successive irrigation practices was proven as an effective approach in alleviating salt stress in a saline-alkali soil. Modification of biochar, known for its porous structure, large surface, and high CEC, with Al further improved its physiochemical properties. Improved properties of AB greatly contributed to the removal of excessive soluble salts, particularly Na^+ ions, from soil exchange sites and soil solution, in turn reducing soil pH and EC. In addition, irrigation practices further enhanced the salt leaching rate. Reduction in salt content led to the improvement in soil physicochemical and biological properties. The underlying mechanism in lowering the salt content with AB application was that Al^{3+} ions in AB possessed a high charge density, which caused the displacement of Na^+ ions from soil exchange sites and allowed them to leach out from soil profile by irrigation water. The Al^{3+} ions also reacted with Na^+ ions in soil solution, forming stable Al-Na complexes that reduced Na^+ availability and resulted in a lower content of Na^+. Moreover, biochar was enriched with nutrients, improving soil structure and nutrient status by releasing multivalent cations after application. Such beneficial changes in soil properties induced positive impacts on the diversity and richness of soil microbial community structure and enzyme activity. The relative abundances of Proteobacteria, Actinobacteriota, Firmicutes, and Chloroflexi were greatly improved, which is important for maintaining soil health. Thus, AB application, in conjunction with irrigation practices, can be considered as an efficient and reliable strategy to reclaim saline-alkali soils.

DECLARATION OF COMPETING INTEREST

The authors declare that they have no known competing financial interests or personal relationships that could have appeared to influence the work reported in this paper.

ACKNOWLEDGEMENT

This study was supported by the National Natural Science Foundation of China (No. 42577377).

SUPPLEMENTARY MATERIAL

Supplementary material for this article can be found in the online version.

REFERENCES

Ablimit R, Li W K, Zhang J D, Gao H N, Zhao Y M, Cheng M M, Meng X Q, An L Z, Chen Y. 2022. Altering microbial community for improving soil properties and agricultural sustainability during a 10-year maize-green manure intercropping in Northwest China. *J Environ Manage*. **321**: 115859.

Adhikari S, Moon E, Timms W. 2024. Identifying biochar production variables to maximise exchangeable cations and increase nutrient availability in soils. *J Clean Prod*. **446**: 141454.

Aide M. 2022. Aluminum soil chemistry: Influence on soil health and forest ecosystem productivity. *Agric Sci*. **13**: 917–935.

Bao S D. 2000. Agricultural Chemical Analysis of Soil (in Chinese). 3rd Edn. China Agricultural Press, Beijing.

Bolan S, Sharma S, Mukherjee S, Kumar M, Rao C S, Nataraj K C, Singh G, Vinu A, Bhowmik A, Sharma H, El-Naggar A, Chang S X, Hou D, Rinklebe J, Wang H L, Siddique K H M, Abbott L K, Kirkham M B, Bolan N. 2024. Biochar modulating soil biological health: A review. *Sci Total Environ*. **914**: 169585.

Cao M Y, Narayanan M, Shi X J, Chen X P, Li Z L, Ma Y. 2023. Optimistic contributions of plant growth-promoting bacteria for sustainable agriculture and climate stress alleviation. *Environ Res*. **217**: 114924.

Che N J, Qu J, Wang J Q, Liu N, Li C L, Liu Y L. 2024. Adsorption of phosphate onto agricultural waste biochars with ferrite/manganese modified-ball-milled treatment and its reuse in saline soil. *Sci Total Environ*. **915**: 169841.

Chen L J, Li C S, Feng Q, Wei Y P, Zheng H, Zhao Y, Feng Y J, Li H Y. 2017. Shifts in soil microbial metabolic activities and community structures along a salinity gradient of irrigation water in a typical arid region of China. *Sci Total Environ*. **598**: 64–70.

Chen M M, Zhang S R, Liu L, Wu L P, Ding X D. 2021. Combined organic amendments and mineral fertilizer application increase rice yield by improving soil structure, P availability and root growth in saline-alkaline soil. *Soil Till Res*. **212**: 105060.

Cui J W, Yang B G, Zhang M L, Song D L, Xu X P, Ai C, Liang G Q, Zhou W. 2023. Investigating the effects of organic amendments on soil microbial composition and its linkage to soil organic carbon: A global meta-analysis. *Sci Total Environ*. **894**: 164899.

Deng Y, Li M, Zhang Z, Liu Q, Jiang K L, Tian J J, Zhang Y, Ni F Q. 2021. Comparative study on characteristics and mechanism of phosphate adsorption on Mg/Al modified biochar. *J Environ Chem Eng*. **9**: 105079.

Ding B X, Cao H X, Zhang J H, Bai Y G, He Z J, Guo S C, Wang B, Jia Z L, Liu H B. 2023. Biofertilizer application improved cotton growth, nitrogen use efficiency, and yield in saline water drip-irrigated cotton fields in Xinjiang, China. *Ind Crops Prod*. **205**: 117553.

Du Y Q, Liu X F, Zhang L, Zhou W. 2023. Drip irrigation in agricultural saline-alkali land controls soil salinity and improves crop yield: Evidence from a global meta-analysis. *Sci Total Environ*. **880**: 163226.

Duan M L, Yan R P, Wang Q J, Zhou B B, Zhu H Y, Liu G H, Guo X, Zhang Z S. 2023. Integrated microbiological and metabolomics analyses to understand the mechanism that allows modified biochar to affect the alkalinity of saline soil and winter wheat growth. *Sci Total Environ*. **866**: 161330.

Ebrahimi-Zarandi M, Etesami H, Glick B R. 2023. Fostering plant resilience to drought with Actinobacteria: Unveiling perennial allies in drought stress tolerance. *Plant stress*. **10**: 100242.

Elmeknassi M, Elghali A, de Carvalho H W P, Laamrani A, Benzaazoua M. 2024. A review of organic and inorganic amendments to treat saline-sodic soils: Emphasis on waste valorization for a circular economy approach. *Sci Total Environ*. **921**: 171087.

Feng Q J, Cao S L, Liao S J, Wassie M, Sun X Y, Chen L, Xie Y. 2023. *Fusarium equiseti*-inoculation altered rhizosphere soil microbial community, potentially driving perennial ryegrass growth and salt tolerance. *Sci Total Environ*. **871**: 162153.

Gao G, Yan L, Tong K Q, Yu H L, Lu M, Wang L, Niu Y S. 2024. The potential and prospects of modified biochar for comprehensive management of salt-affected soils and plants: A critical review. *Sci Total Environ*. **912**: 169618.

Gaudel G, Xing L, Shrestha S, Poudel M, Sherpa P, Raseduzzaman M, Zhang X F. 2024. Microbial mechanisms regulate soil organic carbon mineralization under carbon with varying levels of nitrogen addition in the above-treeline ecosystem. *Sci Total Environ*. **917**: 170497.

Haj-Amor Z, Araya T, Kim D G, Bouri S, Lee J, Ghiloufi W, Yang Y R, Kang H, Jhariya M K, Banerjee A, Lal R. 2022. Soil salinity and its associated effects on soil microorganisms, greenhouse gas emissions, crop yield, biodiversity and desertification: A review. *Sci Total Environ*. **843**: 156946.

Hameed R, Abbas A, Li G L, Shahani A A A, Roha B, Du D L. 2024. Biochar as a soil amendment for saline soils reclamation: Mechanisms and efficacy. *In* Singh S V, Mandal S, Meena R S, Chaturvedi S, Govindaraju K (eds.) Biochar Production for Green Economy. Elsevier, Amsterdam. pp. 205–225.

Han M X, Zhang J S, Zhang L, Wang Z G. 2023. Effect of biochar addition on crop yield, water and nitrogen use efficiency: A meta-analysis. *J Clean Prod*. **420**: 138425.

He K, Xu Y, He G, Zhao X H, Wang C P, Li S J, Zhou G K, Hu R B. 2023. Combined application of acidic biochar and fertilizer synergistically enhances *Miscanthus* productivity in coastal saline-alkaline soil. *Sci Total Environ*. **893**: 164811.

He X, Jiang J, Hong Z N, Pan X Y, Dong Y, Xu R K. 2020. Effect of aluminum modification of rice straw-based biochar on arsenate adsorption. *J Soils Sediments*. **20**: 3073–3082.

Huang W H, Chang Y J, Wu R M, Chang J S, Chuang X Y, Lee D J. 2023. Type-wide biochars loaded with Mg/Al layered double hydroxide as adsorbent for phosphate and mixed heavy metal ions in water. *Environ Res*. **224**: 115520.

Lee X, Yang F, Xing Y, Huang Y M, Xu L, Liu Z T, Holtzman R, Kan I, Li Y L, Zhang L K, Zhou H. 2022. Use of biochar to manage soil salts and water: Effects and mechanisms. *Catena*. **211**: 106018.

Li C Y, Wang Z C, Xu Y T, Sun J F, Ruan X Y, Mao X W, Hu X Y, Liu P. 2023. Analysis of the effect of modified biochar on saline-alkali soil remediation and crop growth. *Sustainability*. **15**: 5593.

Li H, Wang B J, Siri M, Liu C, Feng C L, Shao X Q, Liu K S. 2023. Calcium-modified biochar rather than original biochar decreases salinization indexes of saline-alkaline soil. *Environ Sci Pollut Res*. **30**: 74966–74976.

Li Q N, Liang W Y, Liu F, Wang G H, Wan J, Zhang W, Peng C, Yang J. 2022. Simultaneous immobilization of arsenic, lead and cadmium by magnesium-aluminum modified biochar in mining soil. *J Environ Manage*. **310**: 114792.

Li Y, Nie C, Liu Y H, Du W, He P. 2019. Soil microbial community composition closely associates with specific enzyme activities and soil carbon chemistry in a long-term nitrogen fertilized grassland. *Sci Total Environ*. **654**: 264–274.

Liang J P, Li Y, Si B C, Wang Y Z, Chen X G, Wang X F, Chen H R, Wang H R, Zhang F C, Bai Y G, Biswas A. 2021. Optimizing biochar application to improve soil physical and hydraulic properties in saline-alkali soils. *Sci Total Environ*. **771**: 144802.

Lin H, Liu C J, Li B, Dong Y B. 2021. *Trifolium repens* L. regulated phytoremediation of heavy metal contaminated soil by promoting soil enzyme activities and beneficial rhizosphere associated microorganisms. *J Hazard Mater*. **402**: 123829.

Lin Y C, Yu C L, Zhang Y B, Lu L, Xu D, Peng X L. 2024. Biochar modification methods and mechanisms for salt-affected soil and saline-alkali soil improvement: A review. *Soil Use Manage*. **40**: e12992.

Liu X Q, Yan F L, Wu L F, Zhang F C, Yin F H, Abdelghany A E, Fan J L, Xiao C, Li J B, Li Z J. 2023. Leaching amount and timing modified the ionic composition of saline-alkaline soil and increased seed cotton yield under mulched drip irrigation. *Field Crops Res*. **299**: 108988.

Liu Z X, Gu H D, Yao Q, Jiao F, Hu X J, Liu J J, Jin J, Liu X B, Wang G H. 2024. Soil pH and carbon quality index regulate the biogeochemical cycle couplings of carbon, nitrogen and phosphorus in the profiles of Isohumosols. *Sci Total Environ*. **922**: 171269.

Lu Y, Gu K, Shen Z T, Tang C S, Shi B, Zhou Q Y. 2023. Biochar implications for the engineering properties of soils: A review. *Sci Total Environ*. **888**: 164185.

Mandal S, Pu S Y, Adhikari S, Ma H, Kim D H, Bai Y C, Hou D Y. 2021. Progress and future prospects in biochar composites: Application and reflection in the soil environment. *Crit Rev Environ Sci Technol*. **51**: 219–271.

Navarro-Torre S, Garcia-Caparrós P, Nogales A, Abreu M M, Santos E, Cortinhas A L, Caperta A D. 2023. Sustainable agricultural management of saline soils in arid and semi-arid Mediterranean regions through halophytes, microbial and soil-based technologies. *Environ Exp Bot*. **212**: 105397.

Ouhadi V R, Goodarzi A R. 2006. Assessment of the stability of a dispersive soil treated by alum. *Eng Geol*. **85**: 91–101.

Pandey D, Daverey A, Arunachalam K. 2020. Biochar: Production, properties and emerging role as a support for enzyme immobilization. *J Clean Prod*. **255**: 120267.

Patrick M E, Young C T, Zimmerman A R, Ziegler S E. 2022. Mineralogic controls are harbingers of hydrological controls on soil organic matter content in warmer boreal forests. *Geoderma*. **425**: 116059.

Peng C, Gong K L, Li Q N, Liang W Y, Song H H, Liu F, Yang J, Zhang W. 2023. Simultaneous immobilization of arsenic, lead, and cadmium in soil by magnesium-aluminum modified biochar: Influences of organic acids, aging, and rainfall. *Chemosphere*. **313**: 137453.

Peng Y T, Chen Q, Guan C Y, Yang X, Jiang X Q, Wei M, Tan J F, Li X Y. 2023. Metal oxide modified biochars for fertile soil management: Effects on soil phosphorus transformation, enzyme activity, microbe community, and plant growth. *Environ Res*. **231**: 116258.

Peng Y T, Zhang B G, Guan C Y, Jiang X Q, Tan J F, Li X Y. 2022. Identifying biotic and abiotic processes of reversing biochar-induced soil phosphorus leaching through biochar modification with MgAl layered (hydr)oxides. *Sci Total Environ*. **843**: 157037.

Phuong Tran T C, Nguyen T P, Nguyen Nguyen T T, Thao Tran T N, Hang Nguyen T A, Tran Q B, Nguyen X C. 2021. Enhancement of phosphate adsorption by chemically modified biochars derived from *Mimosa pigra* invasive plant. *Case Stud Chem Environ Eng*. **4**: 100117.

Porras R C, Hicks Pries C E, McFarlane K J, Hanson P J, Torn M S. 2017. Association with pedogenic iron and aluminum: Effects on soil organic carbon storage and stability in four temperate forest soils. *Biogeochemistry*. **133**: 333–345.

Qadir M, Sposito G, Smith C J, Oster J D. 2021. Reassessing irrigation water quality guidelines for sodicity hazard. *Agric Water Manage*. **255**: 107054.

Qian L B, Chen B L. 2014. Interactions of aluminum with biochars and oxidized biochars: Implications for the biochar aging process. *J Agric Food Chem*. **62**: 373–380.

Rahmanian M, Khadem A. 2024. The effects of biochar on soil extra and intracellular enzymes activity. *Biomass Convers Biorefinery*. **14**: 21993–22005.

Ramírez P B, Fuentes-Alburquenque S, Díez B, Vargas I, Bonilla C A. 2020. Soil microbial community responses to labile organic carbon fractions in relation to soil type and land use along a climate gradient. *Soil Biol Biochem*. **141**: 107692.

Sahab S, Suhani I, Srivastava V, Chauhan P S, Singh R P, Prasad V. 2021. Potential risk assessment of soil salinity to agroecosystem sustainability: Current status and management strategies. *Sci Total Environ*. **764**: 144164.

Saifullah, Dahlawi S, Naeem A, Rengel Z, Naidu R. 2018. Biochar application for the remediation of salt-affected soils: Challenges and opportunities. *Sci Total Environ*. **625**: 320–335.

Sánchez E, Zabaleta R, Fabani M P, Rodriguez R, Mazza G. 2022. Effects of the amendment with almond shell, bio-waste and almond shell-based biochar on the quality of saline-alkali soils. *J Environ Manage*. **318**: 115604.

Sharma U, Rawat D, Mukherjee P, Farooqi F, Mishra V, Sharma R S. 2023. Ecological life strategies of microbes in response to antibiotics as a driving factor in soils. *Sci Total Environ*. **854**: 158791.

Siedt M, Schäffer A, Smith K E C, Nabel M, Rob-Nickoll M, van Dongen J T. 2021. Comparing straw, compost, and biochar regarding their suitability as agricultural soil amendments to affect soil structure, nutrient leaching, microbial communities, and the fate of pesticides. *Sci Total Environ*. **751**: 141607.

Singh P, Rawat S, Jain N, Bhatnagar A, Bhattacharya P, Maiti A. 2023. A review on biochar composites for soil remediation applications: Comprehensive solution to contemporary challenges. *J Environ Chem Eng*. **11**: 110635.

Tian Y, Xia R M, Ying Y Q, Lu S G. 2023. Desulfurization steel slag improves the saline-sodic soil quality by replacing sodium ions and affecting soil pore structure. *J Environ Manage*. **345**: 118874.

Wang J Y, Muhammad R, Babar S, El-Desouki Z, Li Y X, Wang X L, Xia X Y, Jiang C C. 2025. Insight into amelioration effect of iron-modified biochar on saline-alkali soil chemical properties and bacterial communities along a soil depth gradient. *Pedosphere*. **35**: 879–892.

Wang J Y, Riaz M, Babar S, Xia H, Li Y X, Xia X Y, Wang X L, Jiang C C. 2023. Iron-modified biochar reduces nitrogen loss and improves nitrogen retention in Luvisols by adsorption and microbial regulation. *Sci Total Environ*. **879**: 163196.

Wang K, Wang S, Zhang X, Wang W Y, Wang X Y, Kong F L, Xi M. 2024. The amelioration and improvement effects of modified biochar derived from *Spartina alterniflora* on coastal wetland soil and *Suaeda salsa* growth. *Environ Res*. **240**: 117426.

Wang X L, Riaz M, Babar S, Eldesouki Z, Liu B, Xia H, Li Y X, Wang J Y, Xia X Y, Jiang C C. 2024a. Alterations in the composition and metabolite profiles of the saline-alkali soil microbial community through biochar application. *J Environ Manage*. **352**: 120033.

Wang X L, Riaz M, Xia X Y, Babar S, El-Desouki Z, Li Y X, Wang J Y, Jiang C C. 2024b. Alleviation of cotton growth suppression caused by salinity through biochar is strongly linked to the microbial metabolic potential in saline-alkali soil. *Sci Total Environ*. **922**: 171407.

Wang Y P, Wang K, Wang X C, Zhao Q L, Jiang J Q, Jiang M. 2024. Effect of different production methods on physicochemical properties and adsorption capacities of biochar from sewage sludge and kitchen waste: Mechanism and correlation analysis. *J Hazard Mater*. **461**: 132690.

Wu L P, Wei C B, Zhang S R, Wang Y D, Kuzyakov Y, Ding X D. 2019. MgO-modified biochar increases phosphate retention and rice yields in saline-alkaline soil. *J Clean Prod*. **235**: 901–909.

Xiao M, Liu G M, Jiang S G, Guan X W, Chen J L, Yao R J, Wang X P. 2022. Bio-organic fertilizer combined with different amendments improves nutrient enhancement and salt leaching in saline soil: A soil column experiment. *Water*. **14**: 4084.

Xu X, Wang J H, Tang Y M, Cui X D, Hou D B, Jia H J, Wang S B, Guo L, Wang J H, Lin A J. 2023. Mitigating soil salinity stress with titanium gypsum and biochar composite materials: Improvement effects and mechanism. *Chemosphere*. **321**: 138127.

Yang C, Chen Y T, Zhang Q, Qie X H, Chen J X, Che Y J, Lv D T, Xu X Y, Gao Y X, Wang Z Y, Sun J. 2023. Mechanism of microbial regulation on methane metabolism in saline-alkali soils based on metagenomics analysis. *J Environ Manage*. **345**: 118771.

Yang F, Xu Z B, Huang Y D, Tsang D C W, Ok Y S, Zhao L, Qiu H, Xu X Y, Cao X D. 2021. Stabilization of dissolvable biochar by soil minerals: Release reduction and organo-mineral complexes formation. *J Hazard Mater*. **412**: 125213.

Yang J, Song Y, Yue Y, Liu W, Che Q, Chen H, Ma H. 2022. Chemically dual-modified biochar for the effective removal of Cr(VI) in solution. *Polymers*. **14**: 10039.

Yin C Y, Zhao J, Chen X B, Li L J, Liu H, Hu Q L. 2022. Desalination characteristics and efficiency of high saline soil leached by brackish water and Yellow River water. *Agric Water Manage*. **263**: 107461.

Yin Q Q, Ren H P, Wang R K, Zhao Z H. 2018. Evaluation of nitrate and phosphate adsorption on Al-modified biochar: Influence of Al content. *Sci Total Environ*. **631-632**: 895–903.

Zhang C, Zhao X, Liang A J, Li Y Y, Song Q Y, Li X Y, Li D P, Hou N. 2023. Insight into the soil aggregate-mediated restoration mechanism of degraded black soil *via* biochar addition: Emphasizing the driving role of core microbial communities and nutrient cycling. *Environ Res*. **228**: 115895.

Zhang G L, Bai J H, Zhai Y J, Jia J, Zhao Q Q, Wang W, Hu X Y. 2024. Microbial diversity and functions in saline soils: A review from a biogeochemical perspective. *J Adv Res*. **59**: 129–140.

Zhang M Y, Riaz M, Liu B, Xia H, El-Desouki Z, Jiang C C. 2020. Two-year study of biochar: Achieving excellent capability of potassium supply *via* alter clay mineral composition and potassium-dissolving bacteria activity. *Sci Total Environ*. **717**: 137286.

Zhang N H, Ye X, Gao Y, Liu G X, Liu Z H, Zhang Q L, Liu E K, Sun S K, Ren X L, Jia Z K, Siddique K H M, Zhang P. 2023. Environment and agricultural practices regulate enhanced biochar-induced soil carbon pools and crop yield: A meta-analysis. *Sci Total Environ*. **905**: 167290.

Zhang P, Bing X, Jiao L, Xiao H, Li B X, Sun H W. 2022. Amelioration effects of coastal saline-alkali soil by ball-milled red phosphorus-loaded biochar. *Chem Eng J*. **431**: 133904.

Zhang S X, Rasool G, Wang S, Zhang Y W, Guo X P, Wei Z J, Zhang X Y, Yang X, Wang T S. 2023. Biochar and *Chlorella* increase rice yield by improving saline-alkali soil physicochemical properties and regulating bacteria under aquaculture wastewater irrigation. *Chemosphere*. **340**: 139850.

Zhang X Q, Qi Y L, Chen Z H, Song N N, Li X, Ren D J, Zhang S Q. 2021. Evaluation of fluoride and cadmium adsorption modification of corn stalk by aluminum trichloride. *Appl Surf Sci*. **543**: 148727.

Zhang Y, Yang J S, Yao R J, Wang X P, Xie W P. 2020. Short-term effects of biochar and gypsum on soil hydraulic properties and sodicity in a saline-alkali soil. *Pedosphere*. **30**: 694–702.

Zhao W, Zhou Q, Tian Z Z, Cui Y T, Liang Y, Wang H Y. 2020. Apply biochar to ameliorate soda saline-alkali land, improve soil function and increase corn nutrient availability in the Songnen Plain. *Sci Total Environ*. **722**: 137428.

Zheng Y L, Zimmerman A R, Gao B. 2020. Comparative investigation of characteristics and phosphate removal by engineered biochars with different loadings of magnesium, aluminum, or iron. *Sci Total Environ*. **747**: 141277.

Zhou M, Liu X B, Meng Q F, Zeng X N, Zhang J Z, Li D W, Wang J, Du W L, Ma X F. 2019. Additional application of aluminum sulfate with different fertilizers ameliorates saline-sodic soil of Songnen Plain in Northeast China. *J Soils Sediments*. **19**: 3521–3533.

Zhou Z X, Li Z Y, Zhang Z Q, You L R, Xu L F, Huang H Y, Wang X P, Gao Y, Cui X J. 2021. Treatment of the saline-alkali soil with acidic corn stalk biochar and its effect on the sorghum yield in western Songnen Plain. *Sci Total Environ*. **797**: 149190.

Zul Azlan Z H, Junaini S N, Bolhassan N A, Wahi R, Arip M A. 2024. Harvesting a sustainable future: An overview of smart agriculture's role in social, economic, and environmental sustainability. *J Clean Prod*. **434**: 140338.